



Particulate Matter Trapping and Oxidation on a Diesel Particulate Filter

Preechar Karin^{1,*} and Katsunori Hanamura¹

¹ Department of Mechanical and Control Engineering, Graduate School of Science and Engineering,
Tokyo Institute of Technology, Tokyo, Japan 152-8552

* Corresponding Author: E-mail. Karin.p.aa@m.titech.ac.jp, Tel/Fax. 81 3 5734 3706

Abstract

Through microscopic visualization experiments, a process generally called “depth filtration” is shown to be caused by surface pores. Also, the existence of a soot cake layer is an important advantage for filtration performance because it can trap most of the particulates. The concept of an ideal diesel particulate filter (DPF), in which a SiC nanoparticle membrane instead of soot cake is sintered on the DPF wall surface, is proposed to improve the filtration performance at the beginning of the trapping process and reduce the energy consumption during the regeneration process. The filtration performance of the membrane filters is shown to be better than that of the conventional DPFs. In the regeneration process, the apparent activation energy for soot oxidation on the membrane filters is smaller than that on the conventional non-catalyst DPFs. The results show that SiC nanoparticles play a significant role in oxygen mobility in soot oxidation territories.

Keywords: Diesel Engine, Emission, Diesel Particulate Filter

1. Introduction

Among internal combustion engines, diesel engines have the highest thermal efficiency. However, particulate matters (PMs) must be removed from exhaust gases that are emitted by diesel engines to protect the environment and human health. Diesel particulate matters (PM) consist of a solid fraction and a soluble organic fraction (SOF). Primary particles, composed of carbon and metallic ash, are coated with SOF and sulfate. The mean diameter of the primary and

agglomerated particles is usually in the range of 20–60 nm and 60–200 nm, respectively. The composition of particles from a diesel engine may vary widely depending on the operating conditions and fuel composition [1–5].

The nanostructures of primary soot particles have been characterized using transmission electron microscopy (TEM) to understand them in detail. A primary soot particle has two distinct parts: an inner core and an outer shell. The inner core has a diameter of



10 nm and it is located at the central region of the primary particle [6, 7].

The electric charge of carbon particles sampled from combustion flames and diesel engines have also been reported. Carbon particles in the later stage of growth are assumed to be charged by thermionic emission and electron capture. The number of charges per particle varies, but averages two. The potential energy increases with increasing charge when the radius of the soot particle is fixed, and decreases with increasing radius for a constant charge [8, 9].

Diesel particulate filters (DPFs) play an important role in particulate trapping and oxidation (regeneration of DPFs). A DPF is generally made of ceramic materials, such as cordierite or silicon carbide, consisting of many rectangular channels with alternate channels blocked using cement at each end. The exhaust gas is forced to flow through a channel wall having numerous micron-scale pores that trap the PM. Furthermore, the collected PM must be oxidized to regenerate the DPF and reduce the back pressure on the diesel engine. A number of studies have been performed to simulate particulate trapping and chemical reactions inside DPFs provide valuable information in designing them [10–12].

Real-time filtration efficiency of DPFs during the trapping process has been measured using a scanning mobility particle sizer and a motor exhaust gas analyzer for particle number analysis and mass analysis, respectively. Results showed that the soot penetration depth into the wall was affected more by particulates characteristics than by filtration velocity [13–15].

Catalytic fuel additives and catalyst DPFs have been proven to reduce the overall activation energy required for particulate oxidation, resulting in lower-temperature oxidation compared to non-catalyst DPFs [16, 17]. The oxidation reaction of soot has been investigated using thermogravimetric analysis and temperature program oxidation to evaluate catalytic activities [18–20]. However, the main problem of catalyzed DPFs for practical use is the low contact area between soot and the active sites of catalyst particles. Thus, the geometry of a DPF wall and the catalyst nanostructures play an important role for efficient regeneration of the filter [21].

Although particulates trapping and oxidation processes involve complex behaviors, very few information is available to aid in understanding such phenomena. However, macro-scale and microscopic visualization of particulates trapping behavior and active regeneration inside a DPF have been investigated successfully to aid in better understanding and future designing of an ideal DPF configuration [22–24].

According to such visualization results, a major problem of conventional DPFs is the filtration performance at the beginning of the trapping process. During this phase, some diesel particulates pass through the DPF wall from the upstream to the downstream side. The amount of particulates trapped increases gradually with time along the shape of the surface pores after the mean pore-scale channels that are connected with the surface pores are blocked by particulates trapped during the initial stage. As a result, filtration performance increases with time,

and most particulates are trapped by the soot cake layer after it develops. As shown in Fig. 1, the surface pores are filled with particulates and only a few particulates, which may have passed through at the beginning of the trapping process, are trapped in the deeper pores. However, the filtration performance decreases again after the DPF is regenerated.

Consequently, the process generally called “depth filtration” is strongly related to the surface pores. The existence of the soot cake layer is also an important advantage for filtration performance because it can trap most particulates.

In the present study, a concept of an ideal DPF, in which a nanosized SiC particle membrane was pasted and sintered on the DPF wall surface instead of soot cake, is proposed to improve the filtration performance (included ultrafine soot particles) at the beginning of the trapping process and to reduce the energy consumption during the regeneration process. The proposed filter is called a diesel particulate membrane filter (DPMF).

2. Experimental Setup and Method

2.1 Microscopic visualization setup

Figure 2 shows a schematic diagram of the experimental setup for microscopic visualization of ultrafine soot particulate trapping and oxidation. A diesel fuel (conventional diesel fuel of JIS K2204 No. 2) lamp was used in the trapping process. Part of the soot inside the diesel flame was introduced into the DPF through a bypass line. The superficial velocity of the inlet gas traveling through the DPF wall was fixed at approximately 12 cm/s.

In the regeneration process, the DPF was regenerated at a maximum temperature of 600 °C (increasing exponentially from 200 °C to 600 °C similar to practical use in actual vehicle) using a high-temperature working gas that was a mixture of nitrogen (93%) and oxygen (7%) and heated by an electric heater. Moreover, the DPF was regenerated at a constant temperature (isothermal) of 525, 550, 575, 600, 625, and

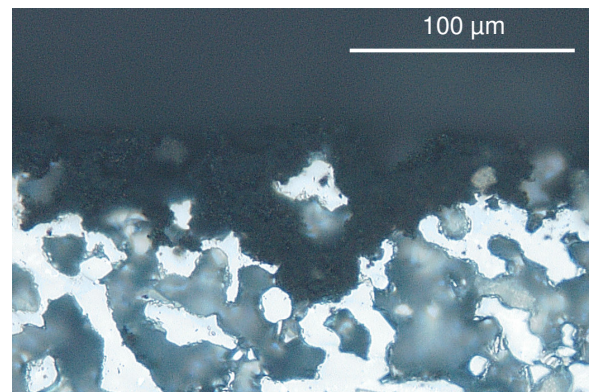


Fig. 1 Optical image of Cross-sectional view of particulate trapping in a conventional DPF.

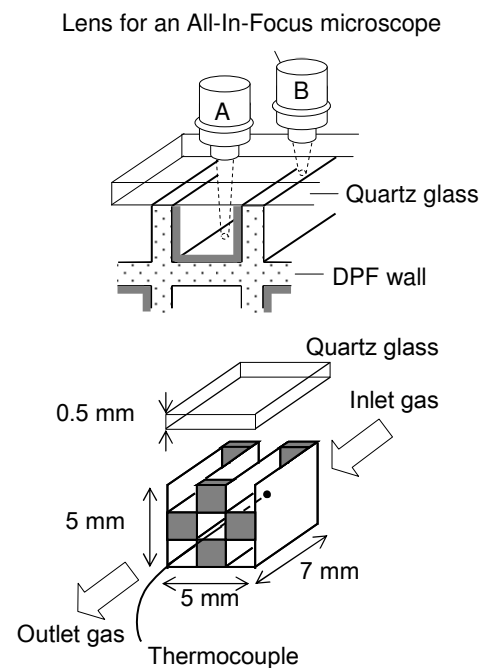


Fig. 2 Experimental setup for microscopic visualization of diesel particulate trapping and oxidation processes [24].

650 °C for the reaction characteristics to compare the apparent activation energies of soot oxidation on each sample. During regeneration, the concentrations of CO and CO₂ emitted from the oxidation reaction of the trapped particulates were measured by an infrared gas analyzer.

2.2 Microstructure of DPFs and DPMFs

Figure 3 shows surface views (left-hand side) and cross-sectional views (right-hand side) of a conventional SiC-DPF with 42% porosity (a) and DPMFs (b), respectively. The DPMF was made of SiC nanoparticles with mixed sizes of 80 nm and 500 nm and sintered onto the conventional SiC-DPF. The DPMF has a thickness of 20 microns and 60% porosity, while the conventional DPF is 300 microns thick and has 42% porosity. The cross-sectional view of the DPMF on the conventional DPF in Fig.3 (b) is very similar to that of the soot cake trapped on it in Fig. 1. In contrast, there are no nanoparticles in the surface pores.

Figure 4 shows SEM images of the membrane filter sintered on the in-flow channel of the conventional SiC-DPF (top) and the fine surface pores (bottom) on the surface of the DPMF. Because the nanoparticles were homogeneously distributed, the mean pore-scale channel size of the membrane (0.5 microns) was smaller than that of the conventional filter (11 microns).

2.3. Micro and nano structures of soot

Figure 5 (a) shows SEM images of diesel particulates emitted by the diesel fuel lamp 5 mm above the bottom end of flame. The uniform micro-scale agglomeration of ultrafine particulates can be clearly seen. The agglomerate size was approximately 100 to 300

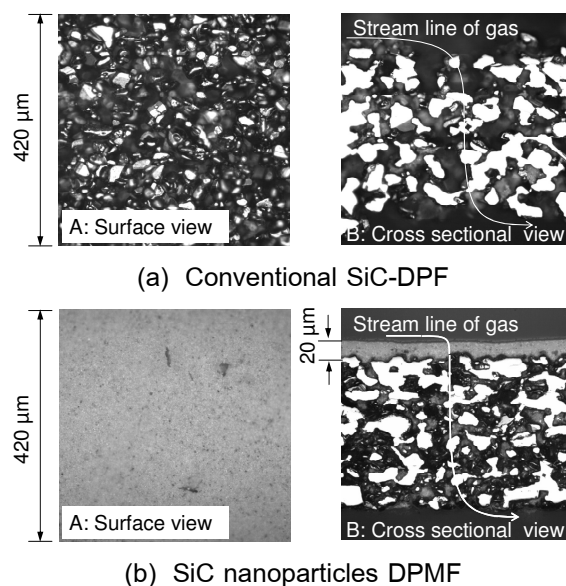


Fig. 3 Optical images of surface and cross-sectional views of the conventional SiC-DPF and SiC nanoparticles DPMF (b), respectively [24].

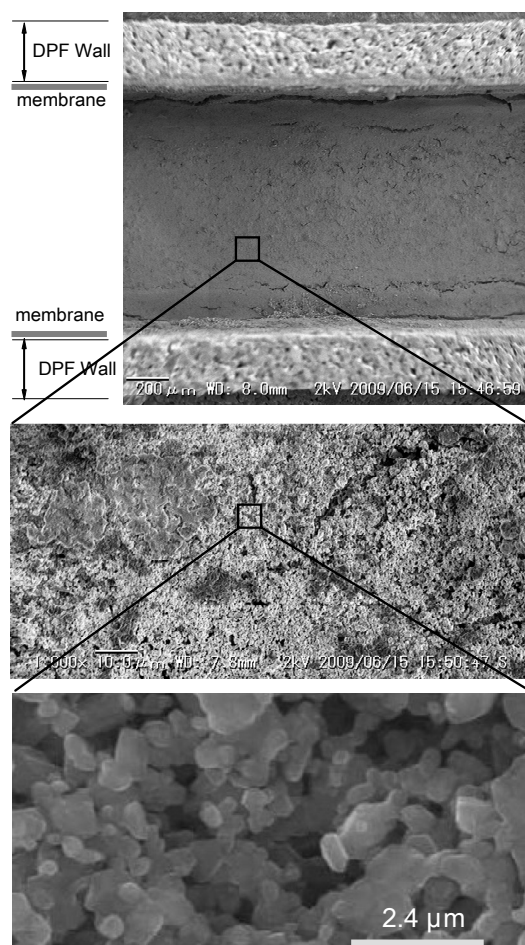


Fig. 4 SEM images of DPMF sintered onto the conventional DPF wall (top) and fine surface pores on the DPMF surface (bottom) [24].

nm and the primary particle size of soot was approximately 20 nm to 60 nm, as shown in Figs. 5 (b) and (c) using TEM. The crystallite of carbon was approximately 3–5 nm × 1 nm in length and thickness, respectively.

2.4. Evaluation of reaction activity

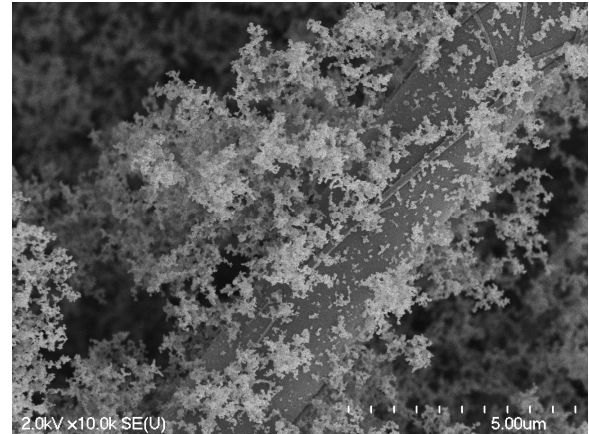
In order to evaluate the reaction activity in the nanoparticle membrane, a comparison between activation energies for reactions of particulates trapped on the membrane and on the conventional DPF was made, where the activation energy was obtained from the production rates of CO and CO₂ and the DPF temperature. Here, the particulates were assumed to react with oxygen resulting in the production of CO and CO₂. The production rate of CO and CO₂ can be expressed as follows:

$$-\frac{d[Y]}{dt} = -k[Y]^n [O_2]^m \quad (1)$$

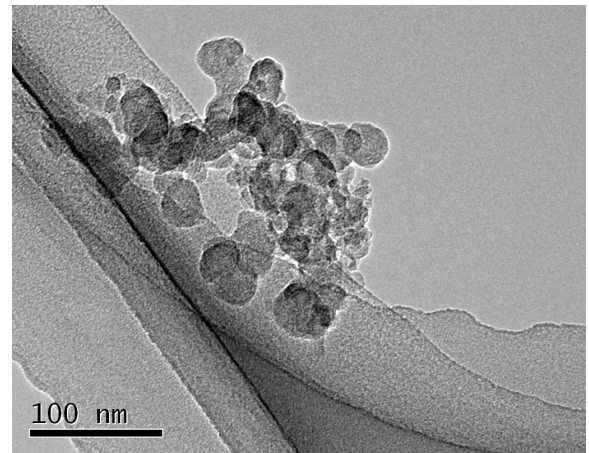
Here, [Y] is the summation of number of remaining moles of carbon at each time step during regeneration. The reaction coefficient k can be described by the Arrhenius-type reaction rate expression. As a result, the activation energy is obtained as the gradient of the following equation:

$$\ln \left[\frac{-1}{[Y]^n} \frac{d[Y]}{dt} \right] = -\frac{E}{RT} + (\ln A + m \ln [O_2]) \quad (2)$$

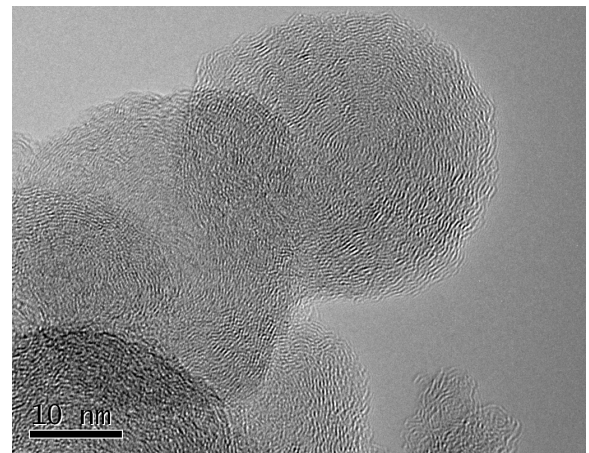
Here, E is the activation energy, R is the gas constant, T is the absolute temperature of the DPF, and the last term on the right-hand side of Eq. (2) is a function of the overall frequency factor and is assumed to be a constant. In this study, the reaction order n was assumed to be 2/3 based on the shrinking core model [18–20].



(a) SEM image of agglomerated soot



(b) TEM image of agglomerated soot



(c) TEM image of primary soot particles

Fig. 5 SEM image (a) and TEM images (b and c) of agglomerates and primary particles of soot emitted by the diesel fuel lamp.

3. Results and Discussion

3.1 Filtration performance

Figure 6 shows SEM images of ultrafine diesel particulates that are captured by glass fiber

filters after passing through the conventional DPF (top) and DPMF (bottom) during 5 minutes of trapping. Note that amount of particulates for the conventional DPF are larger than that of the DPMF. This is because most of the ultrafine diesel particulates can be trapped by the membrane, whereas they pass through the conventional DPF during the beginning of the trapping process.

3.2 Microscopic visualization

Figure 7 shows the time-sequenced surface views during particulate trapping using the conventional DPF with 42% porosity (left) and the DPMF (right). The diesel particulates are first trapped by surface pores on the conventional DPF. Similarly, for DPMF, the diesel particulates are trapped by fine surface pores. Also, a soot cake developed faster than that on the conventional DPF because of the very fine and shallow surface pores.

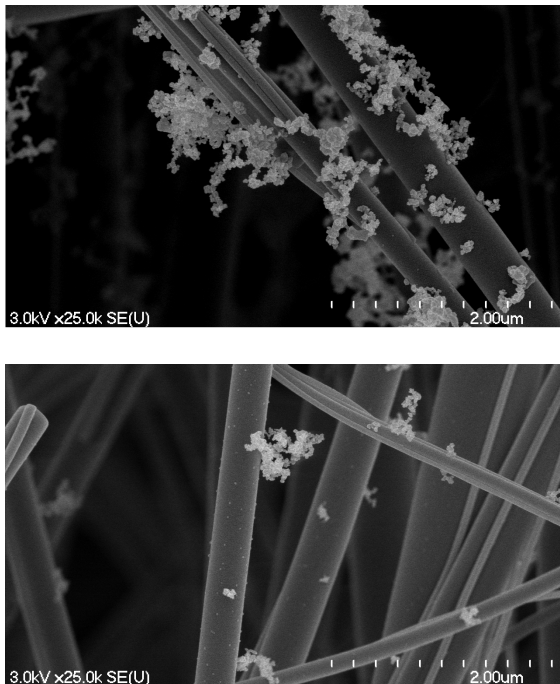


Fig. 6 SEM images of soot captured by glass fiber filters after passing through a conventional DPF (top) and a DPMF (bottom).

Figure 8 shows time-sequenced surface view during particulate matter oxidation. The particulates trapped inside the fine surface pores of the membrane and the large surface pores of the conventional DPF decrease gradually with time along the shape of the pores. These results show that the surface pores play an important role in particulate trapping and oxidation of PM.

3.3 Mechanism of particulate matter trapping

In order to clarify the mechanism of ultrafine particulate matter trapping in the DPF surface pores, the impact of drag (friction), Brownian and electrostatic forces were estimated for better understanding. Figures 9 shows the calculated results of the possible impact of friction, Brownian diffusion and electrostatic forces on a soot particle charged inside the surface pore of the conventional DPF, with 42% porosity and SiC mean particle size of 20 μm , using Stokes–Cunningham's equation, the Einstein's diffusion equation, and Coulomb's law based on conditions of practical use of a vehicle. The average filtration velocity traveling through the surface pores of the conventional DPFs was assumed to be 12 cm/s. The charge on the particles was one charge based on the literature [8, 9].

The root mean square displacement of ultrafine particulates decreases with mean diameter size, even though the Brownian force increase with the size of particles. The root mean square displacement of the primary particulates was larger than the mean pore-scale channels that are connected with the surface pores of the DPFs, especially on the fine surface pores of the DPMFs. It is clearly seen that the drag and Brownian diffusion forces decrease rapidly

when the soot particle size is less than 200 nm, whereas, the electrostatic force increases rapidly. The electrostatic force was larger than the friction force when the particulates were smaller than a mean size of approximately 200 nm.

A possible mechanism for soot trapping on conventional DPFs and DPMFs based on the results of the microscopic visualization and the impact of the drag force, Brownian diffusion, and electrostatic force is as follows. Large amounts

of ultrafine-scale particles could contact the SiC particles surfaces caused by the Brownian motion effect, where the root mean square displacement is on the order of microns. Beyond that distance, the soot particles cannot move because of the electrostatic force between soot particles themselves and between soot particles and the SiC particles; the electrostatic force being larger than the opposing friction force arising from the fluid dynamics of the gas flow.

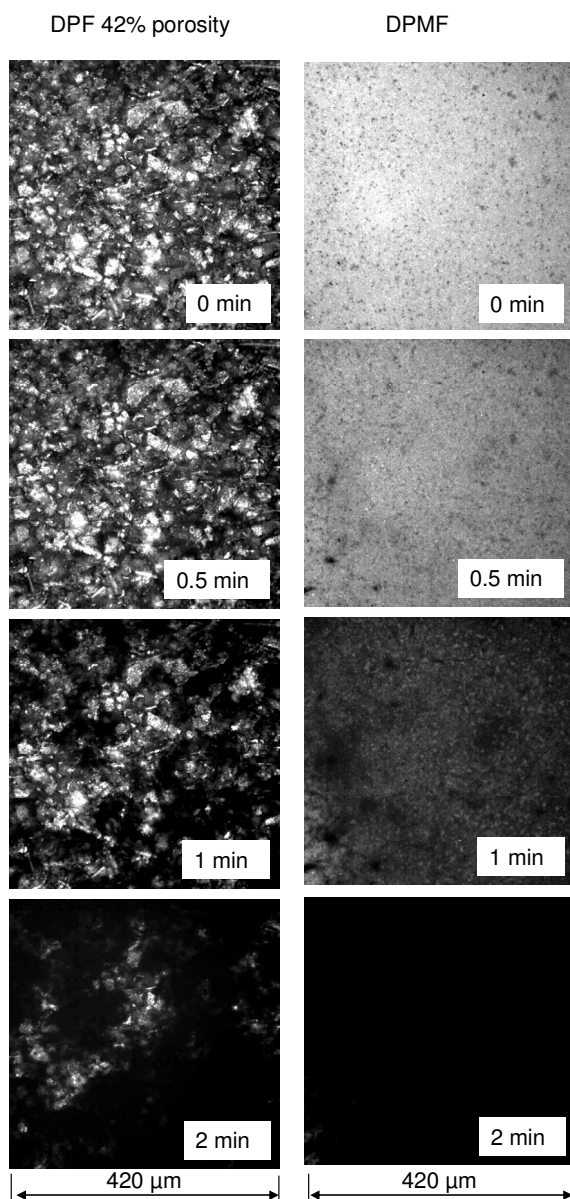


Fig. 7 Optical images of a conventional DPF (left) and DPMF (right) surfaces during the diesel particulate trapping process [25].

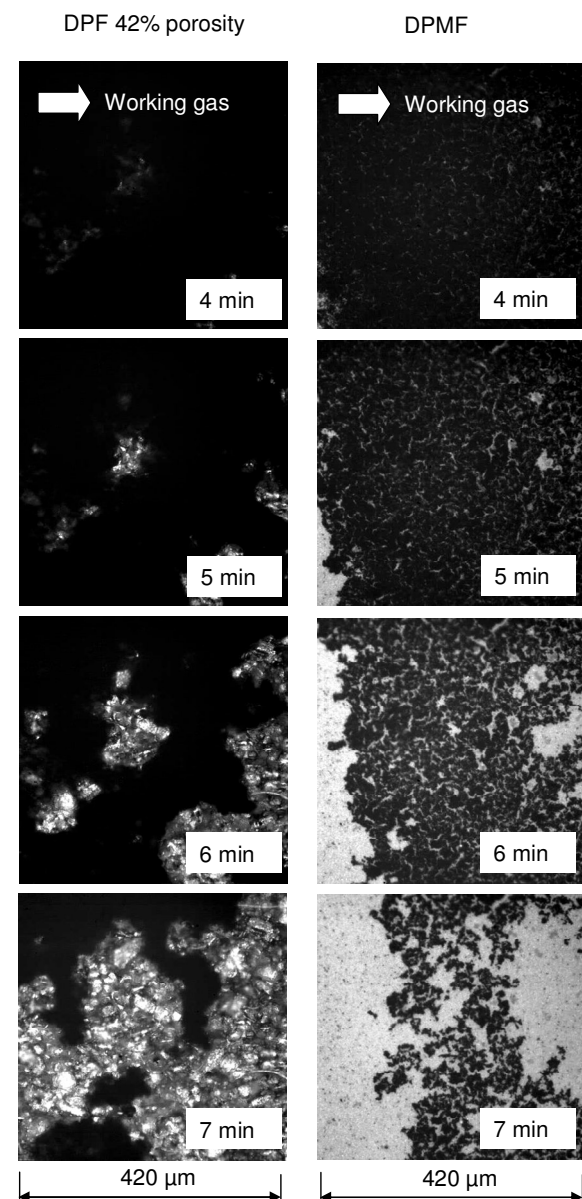


Fig. 8 Optical images of a conventional DPF (left) and DPMF (right) surfaces during the regeneration process [25].

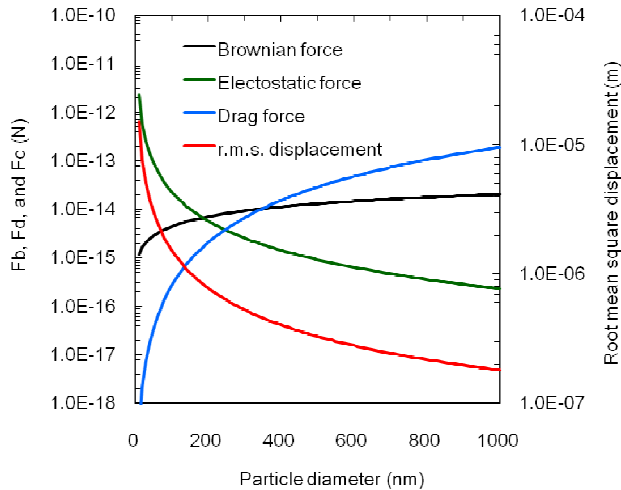


Fig. 9 Results from calculating the impact of Brownian, drag, and electrostatic forces.

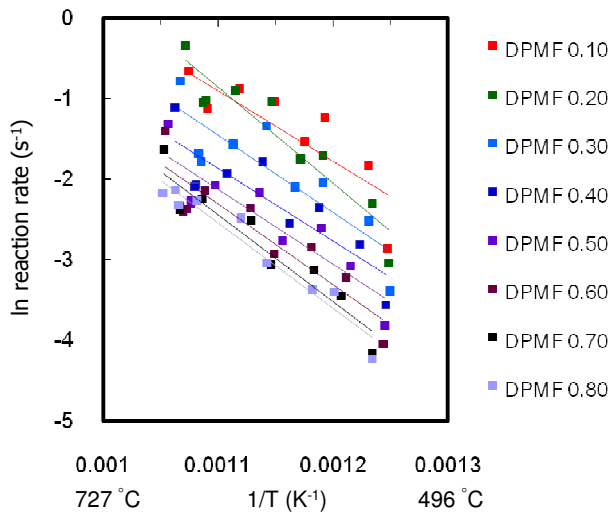


Fig. 10 Arrhenius plot of soot oxidation on the DPMF with respect to soot conversion.

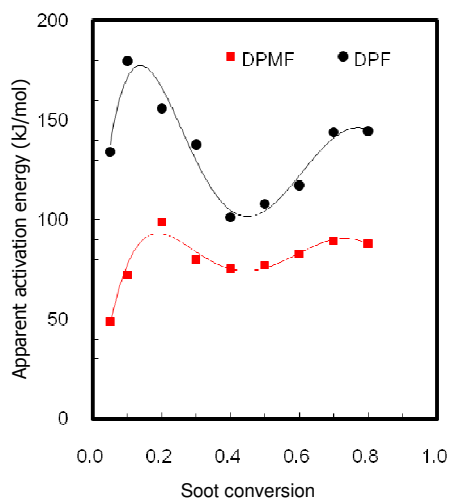


Fig. 11 Apparent activation energy of soot oxidation with respect to soot conversion.

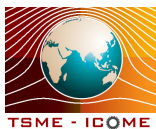
Here, the mean pore-scale channels that connect with the surface pores are blocked by charged particles, leading to the surface pores being filled completely. Finally, the soot cake grows with time. This explains why the soot cake on the DPMFs occurred faster than that on the conventional DPFs, which was because of the membrane's surface pores being very fine and shallow.

3.4 Reaction characteristics

Figure 10 shows the Arrhenius plots used to obtain the apparent activation energy for the DPMF at different conversion levels from 0.1 to 0.8 at each isothermal temperature. Similarly, the conventional DPF was also tested using the same conditions. Figure 11 shows a summary of the apparent activation energy of soot oxidation at each conversion level on the conventional DPF and DPMF. The average apparent activation energy of the conventional non-catalyst DPF and the DPMF were approximately 130 ± 40 and 84 ± 13 kJ/mol, respectively. These results show that the apparent activation energy for the DPMF is lower than the conventional DPF by approximately 36%.

4. Conclusion

In the trapping process, the membrane layer played a significant role because it acted like a soot cake layer. As a result, the ultrafine particulate filtration performance of the DPMFs, even in the beginning of the trapping, was better than that of the conventional DPFs. The ultrafine particulates might have been in contact with the SiC surface near the bottom of each surface pore caused by the Brownian diffusion effect. After that contact occurred, the particulates



could not be removed because of the electrostatic force on the charged particulates.

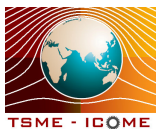
In the regeneration process, the apparent activation energy for oxidation of soot on the DPMFs was smaller than that on the conventional non-catalyst DPFs. As a result, there might have been some catalytic activity for the enhancement of oxidation of the soot layer on the SiC nanoparticles, which are elements of the DPMF. It might be the case that some catalytic activity involving unstable oxides of silicon and/or carbon on the SiC nanoparticle surface caused the high oxygen mobility around the soot oxidation territory.

5. Acknowledgement

The authors gratefully acknowledge support from Honda R&D CO., Ltd, who provided the DPF samples. The authors are grateful to Asumi Ito and Aya Maezawa, undergraduate students in Hanamura laboratory (Research Center for Carbon Recycling and Energy) at the Tokyo Institute of Technology for assistance with the experimental setup and preparing the DPF samples.

6. References

- [1] Heywood, J.B. (1998). Internal Combustion Engine Fundamental, McGraw-Hill series in mechanical engineering, Singapore.
- [2] Smith, O.I. (1981). Fundamentals of soot formation in flames with application to diesel engine particulate emissions, *Progress in Energy and Combustion Science*, Vol. 7, pp.275-291.
- [3] Maricq, M.M. (2007). Review Chemical Characterization of particulate emissions from diesel engine: A review, *Journal of Aerosol Science*, Vol.38, pp.1079-1118.
- [4] Kittelson, D.B. (1998). Engines and nanoparticles: A review, *Journal of Aerosol Science*, Vol.29, pp.575-588.
- [5] Majewski, W.A. and Khair, M.K. (2006). Diesel Emissions and Their Control, SAE Order No.R-303, SAE International. Warrendale USA.
- [6] Ishiguro, T. Takatori, Y. and Akihama, K. (1997). Microstructure of Diesel Soot Particles Probed by Electron Microscopy: First Observation of Inner Core and Outer Shell, *Combustion and Flame*, 108, pp.231-234.
- [7] Vander Wal, R.A. Yezerets, A. Currier, N.W. Kim, D.H. and Wang, C.H. (2007). HRTEM Study of diesel soot collected from diesel particulate filters, *Carbon*, 45, pp.70-77.
- [8] Ball, R.T. and Howard, J.B. (1971). Electric charge of carbon particles in flames, *Symposium (International) on Combustion*, Vol.13, Issue 1, pp.353-362.
- [9] Maricq, M.M. (2006). On the electrical charge of motor vehicle exhaust particles, *Journal of Aerosol Science*, Vol.37, pp.858-874.
- [10] Konstandopoulos, A.G. Kostoglou, M. Vlachos, N. and Kladopoulos, E. (2005). Progress in Diesel Particulate Filter Simulation, *SAE Technical paper*, 2005-01-0946.
- [11] Konstandopoulos, K.G. Zarvalis, D. Kladopoulou E. and Dolios, L. (2006). A multi-reactor assembly for screening of diesel particulate filters, *SAE Technical paper*, 2006-01-0874.
- [12] Tushima, S. Nakamura, I. Sakashita, S. Hirai, S. and Kitayama, D. (2010). Lattice Boltzmann simulation on particle transport and captured behaviors in a 3d-reconstructed micro porous DPF, *SAE Technical paper*, 2010-01-0534.



- [13] Wirojsakunchai, E. Schroeder, E. Kolodziej, C. Foster, D.E. Schmidt, N. Root, T. Kawai, T. Suga, T. Nevius T. and Kusaka, T. (2007). Detailed diesel exhaust particulate characterization and real-time DPF filtration efficiency measurements during PM filling process, *SAE Technical paper*, 2007-01-0320.
- [14] Merkel, G.A. Cutler, W.A. Tao, T. Chiffey, A. Phillips, P. Twigg M.V. and Walker, A. (2003). New cordierite diesel particulate filter for catalyzed and non-catalyzed applications, *Proceeding of the 9th diesel engine emissions reduction conference*, Newport Rhode Island.
- [15] Yapaulo, R.A. Wirojsakunchai, E. Orita, T. Foster, D.E. Akard, M. Walker L.R. and Lance, M.J. (2009). Impact of filtration velocities and particulate matter characteristics on diesel particulate filter wall loading, *International Journal of Engine research*, Professional Engineering Publishing, Vol.10, No.5/2009, pp.287-304.
- [16] Fino, D. and Specchai, V. (2008). Review open issues in oxidative catalysis for diesel particulate abatement, *Powder technology*, Vol.180, pp.64-73.
- [17] Suzuki, J. and Matsumoto, S. (2004). Development of catalysts for diesel particulate NO_x reduction, *Topics in Catalyst*, Vol.28, pp.171-176.
- [18] Neeft, J.P.A. Nijhuis, T.X. Smakman, E. Makkee, M. and Moulijn, J.A. (1997). Kinetics of the oxidation of diesel soot, *Fuel*, Vol.76, No.12, pp.1129-1136.
- [19] Darcy, P. Costa, P.D. Mellottee, H. Trichard J.M. and Mariadassou, G.D. (2007). Kinetics of catalyzed and non-catalyzed oxidation of soot form a diesel engine, *Catalysis Today*, Vol.119, pp.252-256.
- [20] Yezerets, A. Currier, N.W. and Eadler, H.A. (2003). Experimental Determination of the Kinetics of Diesel Soot Oxidation by O₂ – Modeling Consequences, *SAE Technical paper*, 2003-01-0833
- [21] Lorentzou, S. Pagkoura, C. Zygogianni, A. Kastrinaki, G. and Konstandopoulos, A.G. (2008). Catalytic nano-structured materials for next generation diesel particulate filters, *SAE Technical paper*, 2008-01-0417.
- [22] Hanamura, K. Karin, P. Cui, L. Rubio, P. Tsuruta, T. Tanaka, T. and Suzuki, T. (2009). Micro- and macroscopic visualization of particulate matter trapping and regeneration processes in wall-flow diesel particulate filters, *International Journal of Engine research*, Professional Engineering Publishing, Vol.10, No.5/2009, pp.305-321.
- [23] Karin, P. Cui, L. Rubio, P. Tsuruta, T and Hanamura, K. (2009). Microscopic Visualization of PM Trapping and Regeneration in Micro-Structural Pores of a DPF Wall, *SAE International Journal of Fuels and Lubricants*, SAE International, Vol.2, No.1, pp.661-669.
- [24] Karin, P. and Hanamura, K. (2010). Particulate Matter Trapping and Oxidation on Catalyst-Membrane, *SAE International Journal of Fuels and Lubricants*, SAE International, Vol.3, No.1, pp.368-379.
- [25] Karin, P. and Hanamura, K. (2010). Diesel Particulate Matter Trapping and Oxidation on Catalyst Membrane, *2010 JSAE Annual Congress (Spring)*, Society of Automotive Engineers of Japan Inc, No.355-2010-5424.